https://doi.org/10.5194/esurf-2019-41
Preprint. Discussion started: 7 August 2019

Earth Surface Dynamics Discussions
Open Access
EGU

River patterns reveal landscape evolution at the edge of subduction, Marlborough Fault System, New Zealand

Alison R. Duvall[1], Sarah A. Harbert[1], Phaedra Upton[2], Gregory E. Tucker[3], Rebecca M. Flowers[3], and Camille Collett[1*]

[1]Department of Earth and Space Sciences, University of Washington, Seattle, 98195, USA
[2]GNS Science, Lower Hutt, 5040, New Zealand
[3]Department of Geological Sciences, University of Colorado, Boulder, 90309, USA
*now with the Santa Barbara Museum of Natural History

Correspondence to: Alison R. Duvall (aduvall@uw.edu)

Abstract. Here we examine the landscape of New Zealand's Marlborough Fault System, where the Australian and Pacific plates obliquely collide, in order to consider landscape evolution and the controls on fluvial patterns at complicated plate tectonic boundaries. Based on topographic patterns, we divide the study area into two geomorphic domains, the Kaikōura and Inland Marlborough regions. We present maps of drainage anomalies and channel steepness, as well as an analysis of the plan view orientations of rivers and faults, and find abundant evidence of structurally-controlled drainage and a history of capture and rearrangement. Channel steepness is highest in a zone centered on the Kaikōura domain, including within the low-elevation valleys of main stem rivers and at tributaries near the coast. This pattern is consistent with an increase in rock uplift rate toward a subduction front that is locked on its southern end. Based on these results and a wealth of previous geologic studies, we propose two broad stages of landscape evolution over the last 25 million years of orogenesis. In the Kaikōura domain, Miocene folding above blind thrust or reverse faults generated prominent mountain peaks and formed major transverse rivers early in the plate collision history. A transition to Pliocene dextral strike-slip faulting and widespread uplift led to cycles of river channel offset, deflection and capture of tributaries draining across active faults, and headward erosion and captures by major transverse rivers within the Inland Marlborough domain. Despite clear evidence of recent rearrangement of the Inland Marlborough drainage network, rivers in this domain still flow parallel to the older faults, rather than along orthogonal traces of younger, active faults. Continued flow in the established drainage pattern may indicate that younger faults are not yet mature enough to generate the damage and weakening needed to reorient rivers. We conclude that faulting, uplift, river capture and drainage network entrenchment all dictate drainage patterns and that each factor should be considered when assessing tectonic strain from landscapes, particularly at long-lived and complex tectonic boundaries.

https://doi.org/10.5194/esurf-2019-41
Preprint. Discussion started: 7 August 2019

Earth Surface Dynamics Discussions
Open Access
EGU

1 Introduction

Tectonics and deformation impart a lasting impression on landscapes and act as primary drivers of surface processes. Rivers, in particular, are influenced strongly by tectonic forces, as they are affected both by the ensuing mountain uplift (e.g.Whipple and Tucker, 1999; Bishop, 2007) and by material weakening along faults (e.g.Koons, 1995; Molnar et al., 2007; Koons et al., 2012; Roy et al., 2015; 2016a;2016b;2016c). The past few decades of progress in our understanding of fluvial geomorphology in mountainous settings demonstrates the nature of landscapes as archives of orogeny and enables the tracking of tectonics from its surface expression (e.g.Wobus et al., 2006; Whittaker et al., 2008; Cowie et al., 2008, Kirby and Whipple, 2012; Whipple et al., 2013).

Since the early days of river profile analysis (Hack, 1957; 1973; Seeber and Gornitz, 1983, Snow and Slingerland, 1987; Whipple and Tucker, 1999), measures of channel steepness, concavity, and knickpoints have served as the main metrics to resolve uplift and fault-slip histories from the landscape in deforming terrain. Planform patterns of drainage networks, from offset channels (Wallace, 1968) to rivers flowing around or through folds (Keller et al., 1998), can also yield valuable insights into the tectonics underlying the landscape response. The planform rotation of river basins has been used as a marker of crustal strain (Hallet and Molnar, 2001) and to assess the style and rates of off-fault deformation (Goren et al., 2015; Gray et al., 2017). Drainage network morphometry may additionally yield evidence of catchment reorganization of catchments by ridge migration (Pelletier, 2004; Willet et al., 2014) or by whole sale river capture (Craw et al., 2003; Clark et al., 2004; Craw et al., 2013) and flow reversal (Benowitz et al., 2019), often in response to tectonics. Recent studies focusing on fractures in bedrock channels have also revealed the importance of material strength in setting the orientation of rivers (Koons et al., 2012; Roy et al., 2015; 2016a; 2016b; 2016c; Scott and Wohl, 2019). Detailed field and numerical modeling studies of rivers in faulted landscapes demonstrate the sensitivity of fluvial incision to gradients in erodibility between weak fault zones and the surrounding stronger bedrock (Roy et al., 2016c). These studies further show that structurally aligned drainages, with anomalously straight reaches, originate in response to the localization of fluvial erosion along the zones weakened by tectonic strain (Roy et al., 2015; 2016a;2016b).

Despite these advances, many questions remain about the interaction between faults, uplift, erosion, and tectonics, especially at plate boundaries, which experience long-lived and complex deformation fields. How do drainage networks evolve as an orogen deforms and over what timescales do the rivers respond to the changing tectonic boundary conditions? Are patterns in the drainage network overprinted as older faults change and new faults form? How important is the development of topography along faults and the process of river capture in the establishment of structurally aligned drainages? In this contribution, we examine river patterns across the NE South Island, New Zealand's Marlborough Fault System (MFS), at the southern end of the Hikurangi Subduction Zone (Fig. 1). The MFS landscape has evolved in the face of changing oblique Pacific-Australian relative plate motion over the past 25 million years (e.g.King, 2000) and thus offers an excellent case study of how landscapes

https://doi.org/10.5194/esurf-2019-41
Preprint. Discussion started: 7 August 2019

65 record long-lived deformation and in particular, what sets the patterns in drainage networks in complicated tectonic settings. We present analysis of the landscape, including topography, fluvial morphologies in planform and profile, and orientations of rivers as compared to active and inactive faults. We combine these observations with a wealth of existing geologic studies to first assess the long-term landscape evolution of the MFS, and then to discuss the controls of fluvial patterns along complicated plate tectonic boundaries such as this one.

70

2 Geologic Setting

Recent and ongoing deformation within New Zealand results from the oblique convergence of the Australian and Pacific plates (DeMets et al., 2010). This complicated tectonic boundary includes westward oblique subduction of the Pacific plate beneath the Australian plate along the Tonga-Kermadec-Hikurangi trench off the east coast of the North Island and eastward subduction
75 of the Australian plate beneath the Pacific plate along the Puyseguer Trench off the southern coast of the South Island (Fig. 1a). In between, the oblique-dextral Alpine Fault and the ~150 km wide MFS together link these two subduction zones in a broad transform boundary. The MFS, which splays northeastward from the northern end of the Alpine fault, straddles the transition from subduction to oblique continental plate collision. Subduction terminates offshore to the south and east of the Kaikōura peninsula, adjacent to the thinned continental crust of the southward migrating Chatham Rise (Fig. 1a). Geophysical
80 imaging shows that Pacific plate lithosphere extends beneath the MFS (Eberhart-Phillips & Bannister, 2010; Eberhart-Phillips & Reyners, 1997). Prior to the 2016 M_w 7.8 Kaikōura Earthquake, this part of the subduction zone was presumed to be strongly locked and inactive (Eberhart-Phillips & Bannister, 2010). However, InSAR, seismology, and GPS data from this event has reopened debate regarding earthquake activity on the subduction interface (e.g.Hamling et al., 2017; Bai et al., 2017; Wallace et al., 2018; Lanza et al., 2019).

85

Over the ~ 25 Ma lifespan of the Kaikōura orogeny, the Pacific-Australia plate boundary has rotated clockwise and propagated southward (Cande & Stock, 2004; King, 2000; Walcott, 1998), creating a complex and evolving deformation field within the greater Marlborough region, many details of which remain unresolved. At present, plate convergence within the MFS is thought to be taken up primarily on a suite of four parallel mostly dextral faults, the Wairau, Awatere, Clarence and the Hope-
90 Jordan-Kekerengu, that slip at rates of ~5 to 25 mm/yr (Benson et al., 2001; Cowan, 1989; Little et al., 1998; Little & Roberts, 1997; Mason et al., 2006; McCalpin, 1996; Nicol & Van Dissen, 2002; Van Dissen & Yeats, 1991; Wallace et al., 2007, Knuepfer, 1984, 1988; Langridge et al., 2003; 2010, Little et al., 2018, Fig. 2a). In addition to these major faults, several subsidiary reverse and strike-slip faults stretch across the region, both onshore and off, including the 20+ fault strands that ruptured during the 2016 earthquake (Litchfield et al., 2018) (Fig. 1b).

95

Patterns in low-temperature thermochronology point to two general phases of Cenozoic exhumation related to the evolving Pacific-Australia plate boundary in this region. Early in the plate boundary history, deformation may have been focused on a

https://doi.org/10.5194/esurf-2019-41
Preprint. Discussion started: 7 August 2019


Earth Surface Dynamics Discussions Open Access EGU

few important structures that generated topography in the Kaikōura Ranges (Collett et al., 2019; Baker and Seward, 1996). Spatial patterns in apatite and zircon helium ages and thermal modeling reveal Miocene cooling localized to hanging wall rocks, first along the Clarence fault in the Inland Kaikōura Range, then along the Jordan thrust in the Seward Kaikōura Range (Collett et al., 2019). A major influx of coarse Neogene clastic sediment within the Marlborough region (Rattenbury et al., 2006), including the Early Miocene Great Marlborough Conglomerate (Reay, 1993), provides sedimentary evidence of exhumation in response to increased convergence along the plate boundary (Walcott, 1978) and to the emergence of this part of New Zealand above sea level (Browne, 1995). Prior to the development of the current Pacific-Australia plate boundary, much of the New Zealand continent was submerged beneath the ocean (Sutherland, 1999).

Since the late Miocene / early Pliocene, the main Marlborough faults display a primary right-lateral sense of slip with a lesser component of vertical motion. The southwestward migration of the Chatham Rise with respect to the Australian Plate is thought to have driven the southward propagation of dextral faulting (Furlong, 2007; Furlong & Kamp, 2009; Little & Roberts, 1997; Wallace et al., 2007). Estimates of timing, cumulative decrease in total offset, and increase in slip rate suggest dextral motion first on the Awatere fault at ~7 Ma (Little and Jones, 1998), followed by dextral motion on the Clarence fault at ~3 Ma (Browne, 1992), and on the Hope fault by ~1 Ma (Wood et al., 1994). Low-temperature thermochronology shows evidence of uplift and erosion on these and other faults across the region with widespread, rapid exhumation across the eastern MFS starting at ~5 Ma (Collett et al., 2019). Translation of crust along the Marlborough faults into a subduction front termination on its southern end (Little & Roberts, 1997; Walcott, 1998) may have generated vertical block rotations and driven widespread rock uplift and new fault development during this phase of orogeny.

3 Topography and Planform River Patterns

Steep, rugged mountains cover much of the greater Marlborough region (Fig. 1b). The Awatere and Clarence faults form obvious scars across the lower foothills of the eastern range fronts, expressing steep, faceted hillslopes a few hundreds of meters above the main rivers and several kilometers to the west (Fig. 1c blow up image). Based on general patterns in this topography, we divide the study area into two broad geomorphic domains. The exact dividing line between the two domains is somewhat arbitrary but is based on the western limit of distinct topographic ranges that parallel long, straight faults and river valleys. The Kaikōura domain lies to the east and contains the highest peaks (~2.5 km) and the most dramatic relief (Fig. 1d, profiles 1 and 2). Here the parallel Inland and Seaward Kaikōura Ranges construct a dramatic boundary with the sea. These ranges, and a similar swath of mountains just north of the Awatere fault and valley, are separated by the Awatere and Clarence rivers, which flow eastward, parallel to the range fronts, through wide, linear valleys (Fig. 1b).

In the Inland Marlborough domain, elevations are more consistent across the landscape (~1.5 km) and relief is lower in the absence of the valleys and prominent peaks of the Kaikōura Mountains (Fig. 1e, profiles 3 and 4). This domain contains the

https://doi.org/10.5194/esurf-2019-41
Preprint. Discussion started: 7 August 2019

130 headwaters of the Awatere and Clarence rivers. In its upper reaches, the ~400 km long Clarence river flows mainly north to south, flowing across the E-W trending Marlborough faults, before turning east to flow through the Kaikōura domain to the Pacific Ocean (Fig. 1b). The Awatere river flows eastward along its entire course through both domains.

Below we analyze planform trends in the landscape within both geomorphic domains in order to evaluate the fluvial response
135 to Kaikōura orogeny deformation and to assess the main drivers of drainage network patterns.

3.1 Drainage Anomalies

Drainage anomalies, or unusual patterns in river planform, can indicate recent river captures and reorganization of drainage networks, often in response to active tectonics (e.g.Bishop, 1995; Brookfield, 1998; Hallet and Molnar, 2001; Burrato et al.,
140 2003; Clark et al., 2004; Delcaillau et al., 2006; Willett et al., 2014). We mapped drainage anomalies across the study site and found abundant evidence of fluvial disruption within both domains. Following McCalpin (1996) and Craw and Waters (2007), we demarcated river elbows, locations where major rivers take an ~ 90° bend and barbed tributaries, which are channels that join their main river in an upstream rather than downstream direction (Fig. 2b). We also designated water gaps, sections of river that flow across mountain ranges, as well underfit channels, those that appear to have a wider valley geometry than
145 expected for a given discharge (Fig. 2b). These features were mapped using 1:50000 topographic maps from Land Information New Zealand (LINZ), Google Earth imagery, and field observations.

In the Kaikōura domain, the Awatere river takes a relatively straight path northeast to the sea. In contrast, the Clarence river takes multiple sharp bends through this domain, first flowing mainly northeast between the Inland and Seaward Kaikōura
150 ranges before turning sharply to the southeast to cut across the Seaward Kaikōura Range in a water gap. The river then makes two additional sharp turns over a short distance (~12 km), first to the southwest upon exiting the water gap, and then to the southeast to reach the ocean (Fig. 2b). This course suggests that the river flowed northeastward to bypass growing topography, eventually finding a way across the range at its lower, northern end, possibly by exploiting an antecedent stream. The last two bends appear to be in response to right lateral offset along the Kekerengu fault (Fig. 2a), which slips at 24 (+/- 12) mm/yr and
155 has ruptured several times during the Holocene, including during the most recent 2016 earthquake (Little et al., 2018). Similar though smaller magnitude channel offsets occur in many of the first order streams that flow across the Clarence and Awatere faults on the eastern range fronts. Several of these channels are barbed and a few are underfit (Fig. 2b), likely as a result of the processes of lengthening and stream capture in response to local right-lateral motion on the Clarence and Awatere faults (Harbert et al., 2018).

160

In the Inland Marlborough domain, the upper Clarence river and its major tributary, the Acheron river, display numerous sharp bends (Fig. 2b). In the same region, many of the tributary junctions are barbed and suggest that rivers flowed north or west in the past before redirection to the south. In this part of the drainage network, the prevalence of barbed tributaries and river

https://doi.org/10.5194/esurf-2019-41
Preprint. Discussion started: 7 August 2019

elbows indicates a series of captures, possibly by the headward extension of the main Clarence river (McCalpin, 1996). The upper reaches of the Awatere river do not display sharp bends and barbed tributaries of the type observed along the Clarence river. This segment of the river does appear to be underfit (Fig. 2b), an indication that it may have once had a larger upstream area. A small water gap in the headwaters of the Awatere river, along a stream that is also underfit, in the headwaters of the Awatere river (Fig. 2b), could be a previous pathway of the river, if indeed it once had larger headwaters to the west.

A few prominent water gaps exist south of the Hope Fault (Fig. 2b) along rivers that flow through the Hundalee Hills to the Pacific Ocean. This section of the drainage network also flows over many of the fault traces that ruptured during the 2016 Kaikōura earthquake (Fig. 1b).

3.2 Orientations of Rivers and Faults

Hundreds of fault strands, including those of the major Marlborough faults, cross the study area (Fig. 2a). Using the every-direction variogram analysis method, Roy et al. (2016a) quantified topographic anisotropy across the region and demonstrated that drainage patterns reflect this fault network (see their Fig. 8). Building on this previous work, we quantify and compare the orientation of rivers and faults, both active and inactive, using TopoToolbox 2 (Schwanghart and Scherler, 2014) in order to assess the importance of fault development and maturity in dictating the flow path of the drainage network across the two geomorphic domains. The river network was generated from 8m digital elevation data available from the New Zealand government (LINZ, 2012). Faults were compiled from the GNS Science database (Langridge et al., 2016) and are divided into active and inactive categories. To be considered active by GNS Science, the fault must show evidence of movement at least once in the last 100,000 years. For our analysis, we separated the landscape into eight areas: A1 – A8. Areas A1, A4, A7 and A8 are within the Inland Marlborough domain and areas A2, A3, A5, and A6 encompass the Kaikōura domain. Within each area, we computed orientations of individual fault segments from the two activity categories (Fig. 2c) and of river segments of the highest and second-highest Strahler order (Fig. 2d) using network segment and plotting routines contributed to TopoToolbox by Philippe Steer. In our analysis, we normalized the computed orientations of all features by their segment length in order to avoid bias. Results are displayed in half-dial plots showing orientations from 0° (right/east) to 180° (left/west), with 90° (center/north) in the middle of the dial (Fig. 2c;2d).

Results show that within the Kaikōura domain the active and inactive fault orientations overlap strongly and trend NE-SW (Fig 2c). Within A2, A3, and A5, fault segment orientations exhibit a narrower range (~20° and 60°), whereas in A6, faults show a greater degree of variability (Fig. 2c). Within the Inland Marlborough domain, active and inactive faults are clustered into different orientations, with the inactive faults striking more north-south (30° to 90°) and the active faults striking more east-west (0° to 30°) (Fig. 2c). These differences in fault trend are strong enough to influence the compilation plot of all faults (lower right corner, Fig. 2c), which shows a clear distinction between inactive and active fault orientations, similar to the patterns from only the Inland Marlborough domain faults.

https://doi.org/10.5194/esurf-2019-41
Preprint. Discussion started: 7 August 2019


Earth Surface Dynamics Discussions
Open Access
EGU

River orientations also show distinct patterns across the study area. Rivers in the Inland Marlborough domain tend to align more north-south (Fig. 2d), similar to the inactive fault trends (Fig. 2c). In the central Kaikōura domain (A2, A5), the rivers trend NE-SW (Fig. 2d), similar to both the active and inactive faults of this region (Fig. 2c). Areas A3, A6, and A8 include coastal areas that show a wide variety in river orientations, including many channels that drain to the SE, toward the Pacific Ocean (Fig. 2d). Comparison of the All-Rivers compilation with the All-Faults compilation (Fig. 2c,2d lower right corners) shows an overlap in the orientations of both features, the majority of which lie within the 0° to 90° quadrant, with a clustering between 30° and 60°. These patterns are consistent with a structurally-controlled drainage network and the anisotropy analysis of Roy et al. (2016a), which showed differences in orientation and anisotropy strength from east to west across the MFS.

4 River Profiles and Channel Steepness

Empirical studies of bedrock channels in a variety of settings typically show a scaling between local channel slope and upstream drainage area $S=k_s A^{-\theta}$ where S is the local channel gradient, A is the contributing drainage area, and k_s and θ are the channel steepness and concavity indices, respectively (Flint, 1974; Wobus et al., 2006). Channel steepness may vary dramatically from channel to channel, reflecting differences in rock uplift rate and bedrock lithology most commonly (e.g.Snyder et al., 2003; Kirby and Whipple, 2001; Kirby et al., 2003; Duvall et al., 2004; Harkins et al., 2007; Ouimet et al., 2009; DiBiase et al., 2010; Cyr et al., 2014), but also may vary along a single channel profile where an upstream convexity separates channel reaches with different steepness. Channel concavity, θ, on the other hand, is relatively constant among well-adjusted, quasi-equilibrium channels (e.g.Snyder et al., 2003; Kirby and Whipple, 2001; Kirby et al., 2003; Tucker and Whipple, 2002; Duvall et al., 2004; Whipple and Meade, 2004; Wobus et al., 2006; Harkins et al., 2007) but can vary strongly in landscapes that have experienced a complex history of forcing by tectonic, climatic, or lithologic variation (Dorsey and Roering, 2006; Whittaker et al., 2008).

Given the similar climate across the study area and that Torlesse graywacke rocks underlie most of the region (Rattenbury et al., 2006), we interpret spatial variations in MFS river channel indices in the context of spatially-variable uplift and river capture events. However, we recognize that sediment flux, channel width, and changes in climate or geomorphic process through time may also affect the form of channel profiles.

We used the Topographic Analysis Kit (TAK, Forte and Whipple, 2019), which works with TopoToolbox (Shwanghart and Kuhn, 2010; Shwanghart and Scherler, 2014), to generate a batch normalized channel steepness index (k_{sn}) map of the study area (Fig. 3a). K_{sn} is a routinely used measure of channel steepness that accounts for drainages of different profile shape by using a reference channel concavity (Wobus et al., 2006). The batch k_{sn} map shows average k_{sn} values for river segments across the entire studied stream network given a set ‘smoothing distance’ and minimum drainage area. Here we used a

https://doi.org/10.5194/esurf-2019-41
Preprint. Discussion started: 7 August 2019

threshold river drainage area of 5 x 10^6 m^2, a reference concavity of 0.5, and default values for other inputs. For the main Awatere and Clarence rivers, we used the KsnProfiler functionality to make individual distance vs. elevation plots that show k_{sn} and concavity values along sections of each river (Fig. 3b). These river segments were designated manually based on breaks in slope on chi-elevation plots (Perron and Royden, 2013). The k_{sn} values for each of the Awatere and Clarence river segments are superimposed onto the batch steepness map shown as a heavier line weight (Fig. 3a).

Results show k_{sn} values ranging from 0 to 400 m, with the highest values focused in two areas: 1) the northwest corner of the study area and 2) centered on the Kaikōura Ranges (Fig. 3a). The area of high k_{sn} in the northwest corner may be related to rock uplift associated with the restraining bend on the Alpine fault, which lies to the west outside of the figure frame. This region was also heavily glaciated in the past and the high channel steepness may reflect that. The other zone of high k_{sn} exists within the Kaikōura domain, stretching from the Awatere valley to the coast across the Inland and Seaward Kaikōura Ranges and the Papatea Block. This zone of steep rivers overlaps with the highest topographic relief (Fig. 1). We note, however, that the rivers display high k_{sn} values even within the low-elevation main-stem river valleys. Thus, channel patterns are not simply a function of relief.

The region of high k_{sn} within the Kaikōura domain overlaps with the location of widespread, fast Pliocene-to-present exhumation determined from low-temperature thermochronology data (Collett et al., 2019). High k_{sn} also overlaps with the concentrated region of co-seismic vertical deformation that occurred during the 2016 earthquake (Hamling et al., 2017) and with the area underlain by the Pacific Plate (Eberhart-Phillips and Bannister, 2010). Other geomorphic features, such as strath terraces and bedrock exposed along the channels of the Awatere and Clarence rivers, including the stretch of the Clarence river just before it meets the ocean, and flights of marine terraces along the Kaikōura coast, all provide supporting evidence of rapid channel incision and high rates of rock uplift throughout the zone of high k_{sn}. Values of k_{sn} drop off significantly south of the Awatere fault within the Inland Marlborough domain (Fig. 3a).

The spatial patterns in k_{sn}, topography and low-temperature thermochronology indicate an increase in transpression and rock uplift in the Kaikōura domain, toward a subduction front that is locked on its southern end (Little and Roberts, 1997; Walcott, 1998; Eberhart-Phillips and Bannister, 2010; Collett et al., 2019). Longitudinal profiles of the Awatere and Clarence support this hypothesis. Neither the Clarence nor the Awatere display typical concave-up graded profiles. Rather, both rivers are segmented, with lower k_{sn} upper reaches and higher k_{sn} lower reaches. Together, these segments result in an overall straight or slightly convex shape (Fig. 3b), similar to what might be expected for detachment-limited rivers flowing from regions of lower to higher uplift rates (Whipple and Tucker, 1999). The profile segmentation could also relate to drainage capture events (e.g.Yanites et al., 2013; Seagran and Schoenbohm, 2019), such as those proposed to have occurred in the Awatere and Clarence headwaters based on planform patterns (section 3.1).

https://doi.org/10.5194/esurf-2019-41
Preprint. Discussion started: 7 August 2019


Earth Surface Dynamics Discussions
Open Access
EGU

South of the Hope Fault, most rivers have k_{sn} less than 150m, suggestive of lower rates of erosion, and possibly lower rates of uplift. A few sections of river have higher k_{sn} values and steeper river segments can be seen along the watergap crossing the Hundalee Hills (Fig. 3a). These patterns are consistent with coseismic vertical deformation during the 2016 earthquake, which was of a lower magnitude in this region as compared to the norther ruptures (Hamling et al., 2017).

5 Landscape evolution at the edge of Hikurangi subduction

In this section, we link large-scale drainage evolution to the known tectonic and deformation history of the MFS. Based on our analysis of drainage anomalies, channel steepness and fault and river orientations, as well as previously published geologic and thermochronologic data, we propose two general stages of landscape evolution during the Kaikōura orogeny: a relief-development stage from thrusting and mountain building and 2) a channel-offset, headward-erosion, and river-capture stage from oblique dextral faulting and widespread uplift. Below and in Figure 4, we describe the landscape evolution through four approximate time periods to explain the present-day geomorphic domains of the Marlborough region.

Stage 1 In our conceptual model, relief is generated early in the Kaikōura orogeny by range-scale folds built above blind thrust faults within the Kaikōura domain (Van Dissen and Yeats, 1991; Nicol and Van Dissen, 2002). Low-temperature thermochronology analysis suggests that the Inland Kaikōura Range began to form by ~ 25 Ma, and that both the Inland and Seaward Kaikōura Ranges were rising by 15 Ma (Collett et al., 2019). Although thermochronology data is not reported for the Awatere Mountains, we assume a similar, if not earlier development to the Inland Kaikōura Range (Fig. 4a). The ranges were likely built above reactivated structures, possibly Cretaceous normal faults (Crampton et al., 1998; Nicol and Van Dissen, 2002). As the ranges developed, so too did the major transverse rivers, confined between adjacent highlands and flowing parallel to the range fronts in synclinal valleys (Fig. 4a; 4b). Drainage within the Inland Marlborough domain was likely oriented north along inactive faults (Craw et al., 2013).

As deformation progressed into the mid-Miocene, we propose that the once blind reverse faults emerged to the surface, cutting through the previously folded anticline limbs in a manner typical of sequential fold-thrust development (Berg, 1962; Brown, 1983). This model would be consistent with geologic mapping that shows the faults cutting across tilted strata (Rattenbury et al., 2006), and would explain why the faults are not within the major river valleys, at the low-elevation base of the mountain, but rather several hundred meters up the mountain front (Fig. 4b). During this time, Kaikōura domain relief would have increased as hanging wall uplift along reverse faults continued to build the mountains, and both the Awatere and Clarence rivers incised as they accumulated drainage area (Fig. 4b).

https://doi.org/10.5194/esurf-2019-41
Preprint. Discussion started: 7 August 2019


Earth Surface Dynamics Discussions
Open Access
EGU

Stage 2 By the late Miocene / early Pliocene, continued clockwise rotation of the Hikurangi subduction zone (Cande & Stock, 2004; King, 2000; Walcott 1998) led to a widening of the plate boundary and the onset of dextral faulting across the MFS (Knuepfer, 1992; Holt & Haines, 1995; Little & Jones, 1998; Little & Roberts, 1997; Walcott, 1998; Hall et al., 2004; Lamb & Bibby, 1989). Around this time, we interpret the eastern sections of the main Marlborough faults to transition to oblique strike-slip from their earlier thrust or reverse sense of slip (Randall et al., 2011; Lamb, 2011). Rather than inheriting old structures, the strike-slip faults of the western MFS, within the Inland Marlborough domain, may have initiated new faults formed in orientations optimal to accommodate oblique plate convergence. Such a fault history would explain both the change in strike of the active faults by about 15° across the two geomorphic domains (Lamb, 1988; Randall et al., 2011) and the differences in orientation between active and inactive faults in the Inland Marlborough domain, a trend not observed in the Kaikōura domain (Fig. 2c).

In this latest part of the Kaikōura Orogeny, faulting and rock uplift became widespread across the Kaikōura domain, including within low elevation river valleys and at the coast, in addition to continued uplift of the ranges (Collett et al., 2019). Fault segments with a more northerly strike in the Kaikōura domain are more oblique to the plate motion vector and accommodate some contraction even as their primary motion is dextral (Little and Jones, 1998; Nicol and Van Dissen, 2002; Van Dissen & Yeats, 1991). In addition, dextral motion of crust along the Marlborough faults through the Inland Marlborough domain likely drives deformation and crustal thickening along eastern fault terminations in the Kaikōura domain. Seaward translation and overthrusting of crust atop the downgoing subducted slab (Little and Roberts, 1997; Walcott, 1998) is supported by geophysical data that shows a zone of crustal thickening in the overlying plate (Eberhart-Phillips and Bannister, 2010). This pattern of widespread uplift is supported by the k_{sn} map, which shows a hotspot of steep rivers across the Kaikōura domain highlands and lowlands (Fig. 3a).

During this second stage of landscape evolution, we propose that the combination of strike-slip fault motion along major faults, regional uplift, and rapid incision of large rivers maintains relief in the Kaikōura domain and explains the triangular facets bounding the MFS faults, as well as lateral offsets of rivers flowing over strike-slip faults (Fig. 4d). Recent numerical models of strike-slip systems (Duvall and Tucker, 2015; Harbert et al., 2018) with a similar set up of strike-slip faulting and regional uplift (equal uplift on both sides of the fault) show an ongoing cycle of stream-lengthening and capture for tributary channels that drain across strike-slip faults that produces landscapes similar to that of the modern MFS. The modeled landscapes include horizontally offset channels, linear fault valleys running parallel to neighboring high topography, and high-relief steep hillslopes with faceted spurs adjacent to fault strands.

Expansion of the Awatere and Clarence faults westward during this time interval would have disrupted the Inland Marlborough drainage network. Indeed, studies of biological speciation of fish suggest that there was a connection between rivers of the Marlborough region and the Canterbury region to the south until the late Miocene (Craw et al., 2016). In our conceptual model,

https://doi.org/10.5194/esurf-2019-41
Preprint. Discussion started: 7 August 2019

strike-slip fault growth aided the headward erosion of the major rivers in the Kaikōura domain, promoting drainage capture of rivers flowing north (or south) along the old structural grain. We propose that enlargement of upper headwaters through piracy would have happened first along the Awatere River (Fig. 4c) and then along the Clarence River (Fig. 4d). Captures by the Clarence river included the southward deflection of the Acheron, Saxton, and Alma rivers (McCalpin, 1996), a process that we suggest effectively beheaded the Awatere river (Fig. 4d). The underfit nature and low normalized channel steepness of the present-day upper Awatere river (Fig. 2;3) support the idea that it lost a once-greater headwaters.

Others have noted evidence of river captures and drainage reorganization in this region and suggested a history of Clarence catchment drainage rearrangement as recently as the Quaternary (Burridge et al., 2006 to McCalpin 1992; 1996). The convoluted flow path of the main Clarence river (Fig. 2b) suggests that growth may have happened through piecemeal captures and flow reversals of tributary drainages, likely aided by strike-slip faulting and the generation of local relief, as well as other factors, such as the opening of the Hanmer basin around 1 million years ago (Wood et al., 1994) and glacial erosion and deposition during cold phases of the Quaternary.

Southward migration of the Chatham Rise and the consequent propagation of the Hikurangi subduction zone and the overlying MFS (Little and Jones, 1998; Wallace et al., 2007) suggests that active deformation is presently focused at the southern end of the MFS and in the Porters Pass- Amberly zone to the south (Cowan et al., 1996). Continued uplift on the Jordan-Kekerengu, Papatea, and offshore Kaikōura faults could lead to future mountains, water gaps, drainage deflections, and new transverse rivers (Fig. 4d). Uplift and fault activity south of the Hope Fault are already generating topography, water gaps and some steep channels in the Hundalee Hills (Fig. 2b; Fig. 3a). We expect this landscape to evolve further as deformation becomes more focused in this region, possibly leading to through-going strike-slip faults (Cowan et al., 1996) and a hot zone of drainage anomalies and normalized channel steepness similar to the present Marlborough faults landscape.

6 Discussion: Controls on the patterns of drainage networks at long-lived tectonic boundaries

The similarities between orientations of rivers and faults across the study area (Fig. 2) reflects a strong structural control on the geometry of the drainage network (Craw et al., 2013, Roy et al., 2016a). By parsing the active versus inactive faults in the different geomorphic domains, we show that it takes more than simply breaking new faults to redirect drainage. In the earliest phase of the Kaikōura orogeny, when the landmass of the NE end of the South Island was emerging from the sea, many of the rivers may have flowed along or adjacent to inactive faults that once accommodated the rifting of Gondwanaland and/or early Kaikōura orogeny shear. At present, rivers in the Inland Marlborough domain continue to mainly follow the orientation of these older, inactive faults, despite flowing orthogonally over strands of the active Awatere and Clarence strike-slip faults (see the upper Clarence and Acheron Rivers, Fig. 2). This pattern suggests that once rivers establish themselves along a structural grain, they become entrenched and difficult to change, even when exposed to new weakening and tectonic strain.

https://doi.org/10.5194/esurf-2019-41
Preprint. Discussion started: 7 August 2019

360

Numerical modelling by Roy et al. (2016b;2016c) demonstrated the importance of large erodibility gradients between weak zones and intact bedrock for faults or lithologic discontinuities to have an influence on drainage network patterns. The active, strike-slip faults through this domain are likely much younger than the inactive faults. Perhaps then they have not yet experienced enough displacement to produce significant damage (Savage and Brodsky, 2011) and are effectively too immature
365 to influence the strength field and engender drainage realignment. Field measurements of rock material properties from the Henry's Saddle section of the Fowlers fault, a subsidiary of the Awatere fault within the Inland Marlborough domain, show an ~3000 times decrease in cohesion in fault rocks as compared to surrounding intact rocks (Roy et al., 2016c). The authors estimate this difference in rock strength to correspond to an ~80 times increase in erodibility along the fault and note that the drainage in this area tends to follow this weak zone. These observations suggest that fault damage, at least on this section of
370 the Fowler fault, is enough to influence erosion and the drainage network. More comprehensive mapping and quantification of fault damage and bedrock erodibility across the Marlborough faults is required to fully assess the extent of weakening that has occurred with respect to the magnitude needed for widespread reorientation of rivers.

Topography may also be a key factor to the development of a drainage network aligned along the active faults. The ridge-
375 valley topography generated by Miocene thrust-faulting in the Kaikōura domain is absent in the Inland Marlborough domain. There, the active faults are primarily strike-slip and have not generated the fault-parallel, high-relief ranges (Fig.1) that would aide in the development of transverse drainage.

Even if rivers do not presently flow along most of the active faults within the Inland Marlborough domain, these faults still
380 played a role in the drainage network evolution here. Local offset channels and off-fault deformation such as pull apart basins or pressure ridges would have disrupted the local, established drainages, adding vulnerability to capture by the headward-eroding, eastward flowing large rivers.

Within the Kaikōura domain, the active and inactive faults are aligned, likely having rotated together through time, and ridges
385 run parallel to these faults (Fig. 1). As might be expected, the rivers share a similar orientation to these features (Fig. 2d), but notably, neither the main stem of the Clarence or Awatere rivers flows along their namesake active faults. Instead, the river valleys sit hundreds of meters below the faults, which are separated by as much as several kilometres in distance in some locations (Fig. 1c). Tributary channels draining across these faults do manage to flow laterally for several kilometres along or near to the fault traces, but they all eventually carry on to the main rivers (Fig. 2b). Fault-parallel reaches rarely flow for more
390 than the approximate spacing of range-perpendicular drainages before being shortened by river capture from a neighbouring beheaded tributary (Harbert et al., 2018). If the main rivers started flowing in the valleys before the faults daylighted at the surface, as we speculate above (Fig. 4), that would once again indicate the importance of entrenchment of a drainage network and the difficulty of rerouting drainages due to tectonic strain when not starting from a blank slate. Moreover, the issue of

https://doi.org/10.5194/esurf-2019-41
Preprint. Discussion started: 7 August 2019

fault-damage extent and level of rock weakening could also be relevant here, depending on how recently the active strands became exposed at the surface.

7 Conclusions

Fluvial and topographic analysis indicates that the Marlborough landscape evolved by drainage rearrangement from mountain uplift, strike-slip faulting and the headward erosion of main stem rivers during the Kaikoura orogeny. This evolution includes faults in different orientations, some having been reactivated and others newly formed, and ultimately leading to two disparate geomorphic domains. Based on the tectonic and landscape history, we investigated factors that dictate patterns in long-lived drainage networks at oblique convergent plate margins. Our dataset indicates the importance of fault characteristics such as age, displacement and sense of slip, as well as river characteristics, such as incision and entrenchment, headward erosion and capture, in setting patterns in drainage networks, especially within mature landscapes at long-lived tectonic boundaries. We suggest that each of these elements must be considered when trying to glean information about past or present tectonic strain from orientation and patterns of drainage networks, particularly when multiple phases of orogeny are suspected.

8 Acknowledgements

This work was made possible through generous support from the National Science Foundation (grants EAR-132859 and -1321735 to Duvall, Tucker, and Flowers, and -1126991 to Flowers). Upton was supported by the New Zealand Ministry for Business Innovation and Employment (grant C05X1103). Thank you to Phillipe Steere for contributing valuable routines to analyze river orientations in Topotoolbox. We also appreciate valuable discussions with Alex Lechler, Philip Schoettle-Greene, Sean LaHusen, Seth Williams, and Erich Herzig that shaped and improved the paper.

References

Baker, J., and Seward D.: Timing of Cretaceous extension and Miocene compression in northeast South Island, New Zealand: Constraints from Rb-Sr and fission-track dating of an igneous pluton, Tectonics, 15, 976-983, doi:10.1029/96TC00626, 1996.

Bai, Y., Lay, T., Cheung, K.F. and Ye, L.: Two regions of seafloor deformation generated the tsunami for the 13 November 2016, Kaikoura, New Zealand earthquake, Geophys Res Lett, 44, 6597-6606, https://doi.org/10.1002/2017GL073717, 2017.

Benowitz, J.A., Davis, K., and Roeske, S.: A river runs through it both ways across time: $^{40}Ar/^{39}Ar$ detrital and bedrock muscovite geochronology constraints on the Neogene paleodrainage history of the Nenana River system, Alaska Range, Geosphere, 15, doi:10.1130/GES01673.1, 2019.

Benson, A.M., Little, T.A., Van Dissen, R.J., Hill, N. & Townsend, D.B.: Late Quaternary paleoseismic history and surface rupture characteristics of the eastern Awatere strike-slip fault, New Zealand, Geol Soc Am Bull, 113, 1079-1091, doi:10.1130/0016-7606(2001)113<1079:LQPHAS>2.0.CO;2, 2001.

Berg, R.R.: Mountain flank thrusting in Rocky Mountain foreland, Wyoming and Colorado, AAPG Bull, 46, 2019-2032, 1962.

Bishop, P.: Drainage rearrangement by river capture, beheading and diversion, Prog. In Phys Geog: Ea and Env, 19, 449-473, doi:10.1177/030913339501900402, 1995.

Bishop, P.: Long-term landscape evolution: linking tectonics and surface processes, Earth Surf Proc Land, 32, 329-365, doi:10.1002/esp.1493, 2007.

Burrato, P. Ciucci, F., and Valensise, G.: An inventory of river anomalies in the Po Plain, Northern Italy: evidence for active blind thrust faulting, Ann Geophys-Italy, 46, 865–882, 2003.

Burridge, C.P, Craw, D., and Waters, J.M.: River capture, range expansion, and cladogenesis: the genetic signature of freshwater vicariance, Evolution, 16, 1883-1895, doi.org/10.1111/j.0014-3820.2006.tb01181.x, 2006.

Brookfield, M.E.: The evolution of the great river systems of southern Asia during the Cenozoic India-Asia collision: rivers draining southwards, Geomorphology, 22, 285-312, doi.org/10.1016/S0169-555X(97)00082-2, 1998.

Brown, W.G.: Sequential development of the fold-thrust model of foreland deformation, in Lowell, J.D., ed., Rocky Mountain foreland basins and uplifts, Denver, Colorado, Rocky Mountain Association of Geologists, 57-64, 1983.

Browne, G.H.: Sedimentation patterns during the Neogene in Marlborough, New Zealand, J Roy Soc New Zealand, 25, 459-483, doi:10.1080/03014223.1995.9517497, 1995.

Cande, S.C., and Stock, J.M.: Pacific-Antartic-Australia motion and the formation of the Macquarie Plate, Geophys J Int, 157, 399-414, doi:org/10.1111/j.1365-246X.2004.02224.x, 2004.

Clark, M.K., Schoenbohm, L.M., Royden, L.H., Whipple, K.X., Burchfiel, B.C., Zhang, X., Tang, W., Wang, E. and Chen, L.: Surface uplift, tectonics, and erosion of eastern Tibet from large-scale drainage patterns, Tectonics, 23, https://doi.org/10.1029/2002TC001402, 2004.

https://doi.org/10.5194/esurf-2019-41
Preprint. Discussion started: 7 August 2019

Collett, C.M., Duvall, A.R., Flowers, R.M., Tucker, G.E. and Upton, P.: The Timing and Style of Oblique Deformation Within New Zealand's Kaikōura Ranges and Marlborough Fault System Based on Low-Temperature Thermochronology, Tectonics, 38, 1250-1272, https://doi.org/10.1029/2018TC005268, 2019.

Cowan, H.A.: An evaluation of the Late Quaternary displacements and seismic hazard associated with the Hope and Kakapo Faults, Amuri District, North Canterbury, MSc thesis, Univ. of Canterbury, Christchurch, 1989.

Cowan, H., Nicol, A. and Tonkin, P.: A comparison of historical and paleoseismicity in a newly formed fault zone and a mature fault zone, North Canterbury, New Zealand, J Geophys Res-Sol Ea, 101, 6021-6036, https://doi.org/10.1029/95JB01588, 1996.

Cowie, P.A., Whittaker, A.C., Attal, M., Roberts, G., Tucker, G.E. and Ganas, A.: New constraints on sediment-flux–dependent river incision: Implications for extracting tectonic signals from river profiles, Geology, 36, 535-538, https://doi.org/10.1130/G24681A.1, 2008.

Crampton, J.S., Laird, M., Nicol, A., Hollis, C.J. and Van Dissen, R.J.: November. Geology at the northern end of the Clarence Valley, Marlborough; a complete record spanning the Rangitata to Kaikoura orogenies, In Geological Society of New Zealand, New Zealand Geophysical Society 1998 Joint Annual Conference, 30, 1998.

Craw, D. and Waters, J.: Geological and biological evidence for regional drainage reversal during lateral tectonic transport, Marlborough, New Zealand, J Geol Soc, 164, 785-793, https://doi.org/10.1144/0016-76492006-064, 2007.

Craw, D., Nelson, E. and Koons, P.O., Structure and topographic evolution of the Main Divide in the Landsborough-Hopkins area of the Southern Alps, New Zealand, New Zeal J Geol Geop, 46, 553-562, https://doi.org/10.1080/00288306.2003.9515029, 2003.

Craw, D., Upton, P., Walcott, R., Burridge, C. and Waters, J.: Tectonic controls on the evolution of the Clutha River catchment, New Zealand, New Zeal J Geol Geop, 55, 345-359, https://doi.org/10.1080/00288306.2012.709184, 2012.

Craw, D., Upton, P., Horton, T., and Williams, J.: Migration of hydrothermal systems in an evolving collisional orogen, New Zealand, Mineralium Deposita, 48, 233-248, 2013.

https://doi.org/10.5194/esurf-2019-41
Preprint. Discussion started: 7 August 2019

Craw, D., Upton, P., Burridge, C. P., Wallis, G. P., and Waters, J. M.: Rapid biological speciation driven by tectonic evolution in New Zealand, Nat Geosci, 9, 140-144, 2016.

Cyr, A.J., Granger, D.E., Olivetti, V. and Molin, P.: Distinguishing between tectonic and lithologic controls on bedrock channel longitudinal profiles using cosmogenic 10Be erosion rates and channel steepness index, Geomorphology, 209, https://doi.org/10.1016/j.geomorph.2013.12.010, 27-38, 2014.

Delcaillau, B., Carozza, J.-M., and Laville, E.: Recent fold growth and drainage development: the Janauri and Chandigarh anticlines in the Siwalik foothills, northwest India, Geomorphology, 76, 241 – 256, doi:10.1016/j.geomorph.2005.11.005, 2006.

DeMets, C., Gordon, R.G., and Argus, D.F.: Geologically current plate motions, Geophys J Int, 181, 1-80, doi.org/10.1111/j.1365-246X.2009.04491.x, 2010.

DiBiase, R.A., Whipple, K.X., Heimsath, A.M. and Ouimet, W.B.: Landscape form and millennial erosion rates in the San Gabriel Mountains, CA, Earth Planet Sc Lett, 289, 134-144, https://doi.org/10.1016/j.epsl.2009.10.036, 2010.

Dorsey, R.J. and Roering, J.J.: Quaternary landscape evolution in the San Jacinto fault zone, Peninsular Ranges of Southern California: Transient response to strike-slip fault initiation, Geomorphology, 73, 16-32, https://doi.org/10.1016/j.geomorph.2005.06.013, 2006.

Duvall, A.R. and Tucker, G.E.: Dynamic ridges and valleys in a strike-slip environment, J Geophys Res-Earth, 120, 2016-2026, https://doi.org/10.1002/2015JF003618, 2015.

Duvall, A., Kirby, E. and Burbank, D.: Tectonic and lithologic controls on bedrock channel profiles and processes in coastal California, J Geophys Res-Earth, 109, https://doi.org/10.1029/2003JF000086, 2004.

Eberhart-Phillips, D. and Bannister, S.: 3-D imaging of Marlborough, New Zealand, subducted plate and strike-slip fault systems, Geophys. J. Int., 192, 73-96, doi:10.1111/j.1365-246X.2010.04621.x, 2010.

Eberhart-Philips, D., & Reyners, P.: Continental subduction and three-dimensional crustal structure: The northern South Island, New Zealand, J Geophys Res – Sol Ea, 102, 11843-11861, https://doi.org/10.1029/96JB03555, 1997.

Flint, J.J.: Stream gradient as a function of order, magnitude, and discharge, Water Res Res, 10, 969-973,

https://doi.org/10.1029/WR010i005p00969, 1974.

Forte, A.M. and Whipple, K.X.: The Topographic Analysis Kit (TAK) for TopoToolbox, Earth Surf Dynam, *7*, 87-95, https://doi.org/10.5194/esurf-7-87-2019, 2019.

Furlong, K. P.: Locating the deep extent of the plate boundary along the Alpine Fault zone, New Zealand: Implications for patterns of exhumation in the Southern Alps, Special Papers Geological Society of America, 434, doi: 10.1016/j.tecto.2009.04.023, 2007.

Furlong, K. P., and Kamp, P. J.: The lithospheric geodynamics of plate boundary transpression in New Zealand: Initiating and emplacing subduction along the Hikurangi margin, and the tectonic evolution of the Alpine Fault system, Tectonophysics, 474, 449-462, https://doi.org/10.1016/j.tecto.2009.04.023, 2009.

Goren, L., Castelltort, S. and Klinger, Y.: Modes and rates of horizontal deformation from rotated river basins: Application to the Dead Sea fault system in Lebanon, Geology, 43, 843-846, https://doi.org/10.1130/G36841.1**,** 2015.

Gray, H.J., Shobe, C.M., Hobley, D.E., Tucker, G.E., Duvall, A.R., Harbert, S.A. and Owen, L.A.: Off-fault deformation rate along the southern San Andreas fault at Mecca Hills, southern California, inferred from landscape modeling of curved drainages, Geology, 46, 59-62, https://doi.org/10.1130/G39820.1, 2017.

Hack, J.T.: Studies of longitudinal stream profiles in Virginia and Maryland, 294, US Government Printing Office, 1957.

Hack, J.T.: Stream-profile analysis and stream-gradient index, Journal of Research of the us Geological Survey, 1, 421-429, 1973.

Hall, L.S., Lamb, S.H. and Mac Niocaill, C.: Cenozoic distributed rotational deformation, South Island, New Zealand, Tectonics*,* 23*,* doi:10.1029/2002TC001421, 2004.

Hallet, B. and Molnar, P.: Distorted drainage basins as markers of crustal strain east of the Himalaya, J of Geophys Res: Sol Ea, 106, 13697-13709, https://doi.org/10.1029/2000JB900335, 2001.

Hamling, I.J., Hreinsdóttir, S., Clark, K., Elliott, J., Liang, C., Fielding, E., Litchfield, N., Villamor, P., Wallace, L., Wright, T.J. and D'Anastasio, E.: Complex multifault rupture during the 2016 Mw 7.8 Kaikōura earthquake, New Zealand, Science, 356, DOI: 10.1126/science.aam7194, 2017.

https://doi.org/10.5194/esurf-2019-41
Preprint. Discussion started: 7 August 2019

Harbert, S.A., Duvall, A.R. and Tucker, G.E.: The Role of Near-Fault Relief Elements in Creating and Maintaining a Strike-Slip Landscape, Geophys Res Lett, 45, 11-683, https://doi.org/10.1029/2018GL080045, 2018.

Harkins, N., Kirby, E., Heimsath, A., Robinson, R. and Reiser, U.: Transient fluvial incision in the headwaters of the Yellow River, northeastern Tibet, China, J Geophys Res: Earth, 112, https://doi.org/10.1029/2006JF000570, 2007.

Holt, W.E., & Haines, A.J.: The kinematics of northern South Island, New Zealand, determined from geologic strain rates, J Geophys Res – Sol Ea, 100, 17991- 18010, https://doi.org/10.1029/95JB01059, 1995.

Keller, E.A., Zepeda, R.L., Rockwell, T.K., Ku, T.L. and Dinklage, W.S.: Active tectonics at Wheeler ridge, southern San Joaquin valley, California, Geol Soc Am Bull, 110, 298-310, https://doi.org/10.1130/00167606(1998)110<0298:ATAWRS>2.3.CO;2**,** 1998.

King, P.R.: Tectonic reconstructions of New Zealand: 40 Ma to the Present, N. Zealand J. of Geol. and Geophys.*,* 43, 611-638, doi: 10.1080/00288306.2000.9514913, 2000.

Kirby, E. and Whipple, K.X.: Expression of active tectonics in erosional landscapes, J of Struc Geol, 44, 54-75, https://doi.org/10.1016/j.jsg.2012.07.009, 2012.

Kirby, E., Whipple, K.X., Tang, W. and Chen, Z.: Distribution of active rock uplift along the eastern margin of the Tibetan Plateau: Inferences from bedrock channel longitudinal profiles, J Geophys Res: Sol Ea, 108, https://doi.org/10.1029/2001JB000861, 2003.

Knuepfer, P.L.K.: Tectonic geomorphology and present-day tectonics of the Alpine shear system, South Island, New Zealand*,* PhD thesis, 509 pp., University of Arizona, Tucson, 1984.

Knuepfer, P.L.K.: Estimating ages of late Quaternary stream terraces from analysis of weathering rinds and soils, Geol Soc Am Bull, 100, 1224-1236, https://doi.org/10.1130/0016-7606(1988)100<1224:EAOLQS>2.3.CO;2, 1988.

Koons, P.O.: Modeling the topographic evolution of collisional belts, Ann Rev Ear Plan Sci, *23*, 375-408, 1995.

Koons, P.O., Upton, P. and Barker, A.D.: The influence of mechanical properties on the link between tectonic and topographic evolution, Geomorphology, 137, 168-180, https://doi.org/10.1016/j.geomorph.2010.11.012, 2012.

https://doi.org/10.5194/esurf-2019-41
Preprint. Discussion started: 7 August 2019

Lamb, S.: Cenozoic tectonic evolution of the New Zealand plate-boundary zone: A paleomagnetic perspective, Tectonophysics, 509, 135-164. doi:10.1016/j.tecto.2011.06.005, 2011.

Lamb, S.H., and Bibby, H.M.: The last 25 Ma of rotational deformation in part of the New Zealand plate-boundary zone, J Struct Geol, 11, 473-492, https://doi.org/10.1016/0191-8141(89)90024-2, 1989.

Langridge, R., Campbell, J., Hill, N., Pere, V., Pope, J., Pettinga, J., Estrada, B., and Berryman, K.: Paleoseismology and slip rate of the Conway Segment of the Hope Fault at Greenburn Stream, South Island, New Zealand, Ann Geophys, 46, 1119-1139, 2003.

Langridge, R. M., Ries, W. F., Litchfield, N. J., Villamor, P., Van Dissen, R. J., Barrell, D. J. A., Rattenbury, M. S., Heron, D. W., Haubrock, S., Townsend, D. B., Lee, J. M., Berryman, K. R., Nicol, A., Cox, S. C., and Stirling, M. W.: The New Zealand Active Faults Database: New Zeal J Geol Geop, 59, 86-96, https://doi.org/10.1080/00288306.2015.1112818, 2006.

Langridge, R.M., Villamor, P., Basili, R., Almond, P., Martinez-Diaz, J.J., and Canora, C.: Revised slip rates for the Alpine fault at Inchbonnie: Implications for plate boundary kinematics of South Island, New Zealand, Lithosphere, 2, 139-152, doi:10.1130/L88.1, 2010.

Lanza, F., Chamberlain, C.J., Jacobs, K., Warren-Smith, E., Godfrey, H.J., Kortink, M., Thurber, C.H., Savage, M.K., Townend, J., Roecker, S. and Eberhart-Phillips, D.: Crustal fault connectivity of the Mw 7.8 2016 Kaikōura earthquake constrained by aftershock relocations, Geophys Res Lett, https://doi.org/10.1029/2019GL082780, 2019.

Litchfield, N. J., Villamor, P., Dissen, R. J. V., Nicol, A., Barnes, P. M., A. Barrell, D. J., Pettinga, J. R., Langridge, R. M., Little, T. A., Mountjoy, J. J., Ries, W. F., Rowland, J., Fenton, C., Stirling, M. W., Kearse, J., Berryman, K. R., Cochran, U. A., Clark, K. J., Hemphill-Haley, M., Khajavi, N., Jones, K. E., Archibald, G., Upton, P., Asher, C., Benson, A., Cox, S. C., Gasston, C., Hale, D., Hall, B., Hatem, A. E., Heron, D. W., Howarth, J., Kane, T. J., Lamarche, G., Lawson, S., Lukovic, B., McColl, S. T., Madugo, C., Manousakis, J., Noble, D., Pedley, K., Sauer, K., Stahl, T., Strong, D. T., Townsend, D. B., Toy, V., Williams, J., Woelz, S., and Zinke, R.: Surface Rupture of Multiple Crustal Faults in the 2016 Mw 7.8 Kaikōura, New Zealand, Earthquake, B Seismol Soc Am, 108, 1496-1520, https://doi.org/10.1785/0120170300, 2018.

Little, T.A., and Jones, A.: Seven million years of strike-slip and related off-fault deformation, northeastern Marlborough fault system, South Island, New Zealand, Tectonics, 17, 285-302, https://doi.org/10.1029/97TC03148, 1998.

625 Little, T.A., and Roberts, A.P.: Distribution and mechanism of Neogene to present-day vertical axis rotations, Pacific-Australian plate boundary zone, South Island, New Zealand, J of Geophys Res – Sol Ea., 102, 20447-20468, https://doi.org/10.1029/97JB01279, 1997.

Little, T.A., Grapes, R., & Berger, G.W.: Late Quaternary strike slip on the eastern part of the Awatere fault, South Island,
630 New Zealand, Geol Soc Am Bull, 110, 127-148, https://doi.org/10.1130/0016-7606(1998)110<0127:LQSSOT>2.3.CO;2, 1998.

Little, T.A., Van Dissen, R., Kearse, J., Norton, K., Benson, A. and Wang, N.: Kekerengu fault, New Zealand: Timing and size of Late Holocene surface ruptures, B Seismol Soc Am, 108, 1556-1572, https://doi.org/10.1785/0120170152, 2019.

635

Mason, D.P.M., Little, T.A., and Van Dissen, R.J.: Rates of active faulting during late Quaternary fluvial terrace formation at Saxton River, Awatere fault, New Zealand, Geol Soc Am Bull, 118, 1431-1446, https://doi.org/10.1130/B25961.1, 2006.

McCalpin, J.P.: Glacial and postglacial geology near Lake Tennyson, Clarence River, New Zealand, New Zeal J Geol Geop, 35, 201-210, https://doi.org/10.1080/00288306.1992.9514514, 1992.

640 McCalpin, J.P.: Tectonic geomorphology and Holocene paleoseismicity of the Molesworth section of the Awatere Fault, South Island, New Zealand, New Zeal J Geol Geop, 39, doi:10.1080/00288306.1996.9514693, 1996.

Molnar, P., Anderson, R.S. and Anderson, S.P.: Tectonics, fracturing of rock, and erosion, J Geophys Res: Sol Ea, 112, https://doi.org/10.1029/2005JF000433, 2007.

645

Nicol, A., and Van Dissen, R.: Up-dip partitioning of displacement components on the oblique-slip Clarence Fault, N. Zeal. J Struct Geol, 24, 1521-1535, https://doi.org/10.1016/S0191-8141(01)00141-9, 2002.

Ouimet, W.B., Whipple, K.X. and Granger, D.E.: Beyond threshold hillslopes: Channel adjustment to base-level fall in
650 tectonically active mountain ranges, Geology, 37, 579-582, https://doi.org/10.1130/G30013A.1, 2009.

Pelletier, J.D.: Persistent drainage migration in a numerical landscape evolution model, Geophys Res Lett, 31, https://doi.org/10.1029/2004GL020802, 2004.

655 Perron, J.T. and Royden, L.: An integral approach to bedrock river profile analysis, Earth Surf Proc Land, 38, 570-576, https://doi.org/10.1002/esp.3302, 2013.

Randall, K., Lamb, S. & Mac Niocaill, C.: Large tectonic rotations in a wide zone of Neogene distributed dextral shear, northeastern South Island, New Zealand, Tectonophysics, 509, 165-190. doi:10.1016/j.tecto.2011.05.006, 2011.

Rattenbury, M.S., Townsend, D.B., and Johnston, M.R. (compilers): Geology of the Kaikōura Area, Institute of Geological and Nuclear Sciences 1:250000 Geological Map 13, Lower Hutt, New Zealand, GNS Science, 1 sheet + 70 p., 2006.

Reay, M.B.: Geology of the middle Clarence valley, Inst. Of Geol. and Nuc. Sci. geol. map 10, Lower Hutt, Institute of Geol. and Nuc. Sci., 144 p. +1 map, 1993.

Roy, S.G., Koons, P.O., Upton, P. and Tucker, G.E.: The influence of crustal strength fields on the patterns and rates of fluvial incision, J Geophys Res: Earth, 120, 275-299, https://doi.org/10.1002/2014JF003281, 2015.

Roy, S.G., Koons, P.O., Osti, B., Upton, P. and Tucker, G.E.: Multi-scale characterization of topographic anisotropy, Comput Geosci, 90, 102-116, https://doi.org/10.1016/j.cageo.2015.09.023, 2016a.

Roy, S.G., Koons, P.O., Upton, P. and Tucker, G.E.: Dynamic links among rock damage, erosion, and strain during orogenesis, Geology, 44, 583-586, https://doi.org/10.1130/G37753.1, 2016b.

Roy, S.G., Tucker, G.E., Koons, P.O., Smith, S.M. and Upton, P.: A fault runs through it: Modeling the influence of rock strength and grain-size distribution in a fault-damaged landscape, J Geophys Res: Earth, 121, 1911-1930, https://doi.org/10.1002/2015JF003662, 2016c.

Savage, H.M. and Brodsky, E.E.: Collateral damage: Evolution with displacement of fracture distribution and secondary fault strands in fault damage zones, J Geophys Res: Sol Ea, 116, https://doi.org/10.1029/2010JB007665, 2011.

Schwanghart, W. and Kuhn, N.J.: TopoToolbox: A set of Matlab functions for topographic analysis, Environmental Modelling & Software, 25, 770-781, https://doi.org/10.1016/j.envsoft.2009.12.002, 2010.

Schwanghart, W. and Scherler, D.: TopoToolbox 2–MATLAB-based software for topographic analysis and modeling in Earth surface sciences, Earth Surf Dynam, 2, 1-7, DOI:10.5194/esurf-2-1-2014, 2014.

Scott, D.N. and Wohl, E.E.: Bedrock fracture influences on geomorphic process and form across process domains and scales, Earth Surf Proc Land, 44, 27-45, https://doi.org/10.1002/esp.4473, 2019.

Seagren, E.G. and Schoenbohm, L.M.: Base Level and Lithologic Control of Drainage Reorganization in the Sierra de las Planchadas, NW Argentina, J Geophys Res: Earth, https://doi.org/10.1029/2018JF004885, 2019.

Seeber, L. and Gornitz, V.: River profiles along the Himalayan arc as indicators of active tectonics, Tectonophysics, 92, 335-367, https://doi.org/10.1016/0040-1951(83)90201-9, 1983.

Snow, R.S. and Slingerland, R.L.: Mathematical modeling of graded river profiles, J Geol, 95, 15-33, 1987.

Snyder, N.P., Whipple, K.X., Tucker, G.E. and Merritts, D.J.: Importance of a stochastic distribution of floods and erosion thresholds in the bedrock river incision problem, J Geophys Res: Sol Ea, 108, https://doi.org/10.1029/2001JB001655, 2003.

Tucker, G.E. and Whipple, K.X.: Topographic outcomes predicted by stream erosion models: Sensitivity analysis and intermodel comparison, J Geophys Res: Sol Ea, 107, https://doi.org/10.1029/2001JB000162, 2002.

Walcott, R.I.: Present tectonics and late Cenozoic evolution of New Zealand, Geophys J Int, 52, 137-64, https://doi.org/10.1111/j.1365-246X.1978.tb04225.x, 1978.

Walcott, R.I.: Modes of oblique compression: Late Cenozoic tectonics of the South Island of New Zealand, Rev Geophys, 1-26, https://doi.org/10.1029/97RG03084, 1998.

Wallace, L.M., Beavan, J., McCaffrey, R., Berryman, K., and Denys, P.: Balancing the plate motion budget in the South Island, New Zealand using GPD, geological and seismological data, Geophys J Int, 168, 332-352, doi:10.1111/j.1365-246X.2006.03183.x, 2007.

Wallace, L.M., Hreinsdóttir, S., Ellis, S., Hamling, I., D'Anastasio, E. and Denys, P.: Triggered slow slip and afterslip on the southern Hikurangi subduction zone following the Kaikōura earthquake, Geophys Res Lett, 45, 4710-4718, https://doi.org/10.1002/2018GL077385, 2018.

Wallace, R.E.: Notes on stream channels offset by the San Andreas fault, southern Coast Ranges, California. In Conference on Geologic Problems of the San Andreas Fault System. Stanford University Publication in Geological Sciences, 11, 6-21, 1968.

Whipple, K.X. and Meade, B.J.: Controls on the strength of coupling among climate, erosion, and deformation in two-sided, frictional orogenic wedges at steady state, J Geophys Res: Earth, 109, https://doi.org/10.1029/2003JF000019, 2004.

https://doi.org/10.5194/esurf-2019-41
Preprint. Discussion started: 7 August 2019

Whipple, K. X. and Tucker, G. E.: Dynamics of the stream-power river incision model: Implications for height limits of mountain ranges, landscape response timescales, and research needs, J Geophys Res: Sol Ea, 104, 17661–17674, doi:10.1029/1999JB900120, 1999.

Whipple, K.X., Dibiase, R.A. and Crosby, B.T.: Bedrock rivers, In Treatise on geomorphology, 550–573, Elsevier Inc, 2013.

Whittaker, A.C., Attal, M., Cowie, P.A., Tucker, G.E. and Roberts, G.: Decoding temporal and spatial patterns of fault uplift using transient river long profiles, Geomorphology, 100, 506-526, https://doi.org/10.1016/j.geomorph.2008.01.018, 2008.

Willett, S.D., McCoy, S.W., Perron, J.T., Goren, L. and Chen, C.Y.: Dynamic reorganization of river basins, Science, 343, DOI: 10.1126/science.1248765, 2014.

Wobus, C., Whipple, K.X., Kirby, E., Snyder, N., Johnson, J., Spyropolou, K., Crosby, B., Sheehan, D. and Willett, S.D.: Tectonics from topography: Procedures, promise, and pitfalls, Special papers – Geol Soc Am, 398, pp.55, 2006.

Wood, R.A., Pettinga, J.R., Bannister, S., Lamarche, G., and McMorron, T.J: Structure of the Hanmer strike-slip basin, Hope fault, New Zealand, Geol Soc Am Bull, 106, 1459-1473, https://doi.org/10.1130/0016-7606(1994)106<1459:SOTHSS>2.3.CO;2**,** 1994.

Van Dissen, R., and Yeats, R.S.: Hope fault, Jordan thrust, and uplift of the Seaward Kaikōura Range, New Zealand, Geology, 19, 393-396, https://doi.org/10.1130/0091-7613(1991)019<0393:HFJTAU>2.3.CO;2**,** 1991.

Yanites, B.J., Ehlers, T.A., Becker, J.K., Schnellmann, M. and Heuberger, S.: High magnitude and rapid incision from river capture: Rhine River, Switzerland, J Geophys Res: Earth, 118, 1060-1084, https://doi.org/10.1002/jgrf.20056, 2013.

https://doi.org/10.5194/esurf-2019-41
Preprint. Discussion started: 7 August 2019

Earth Surface Dynamics Discussions
Open Access
EGU

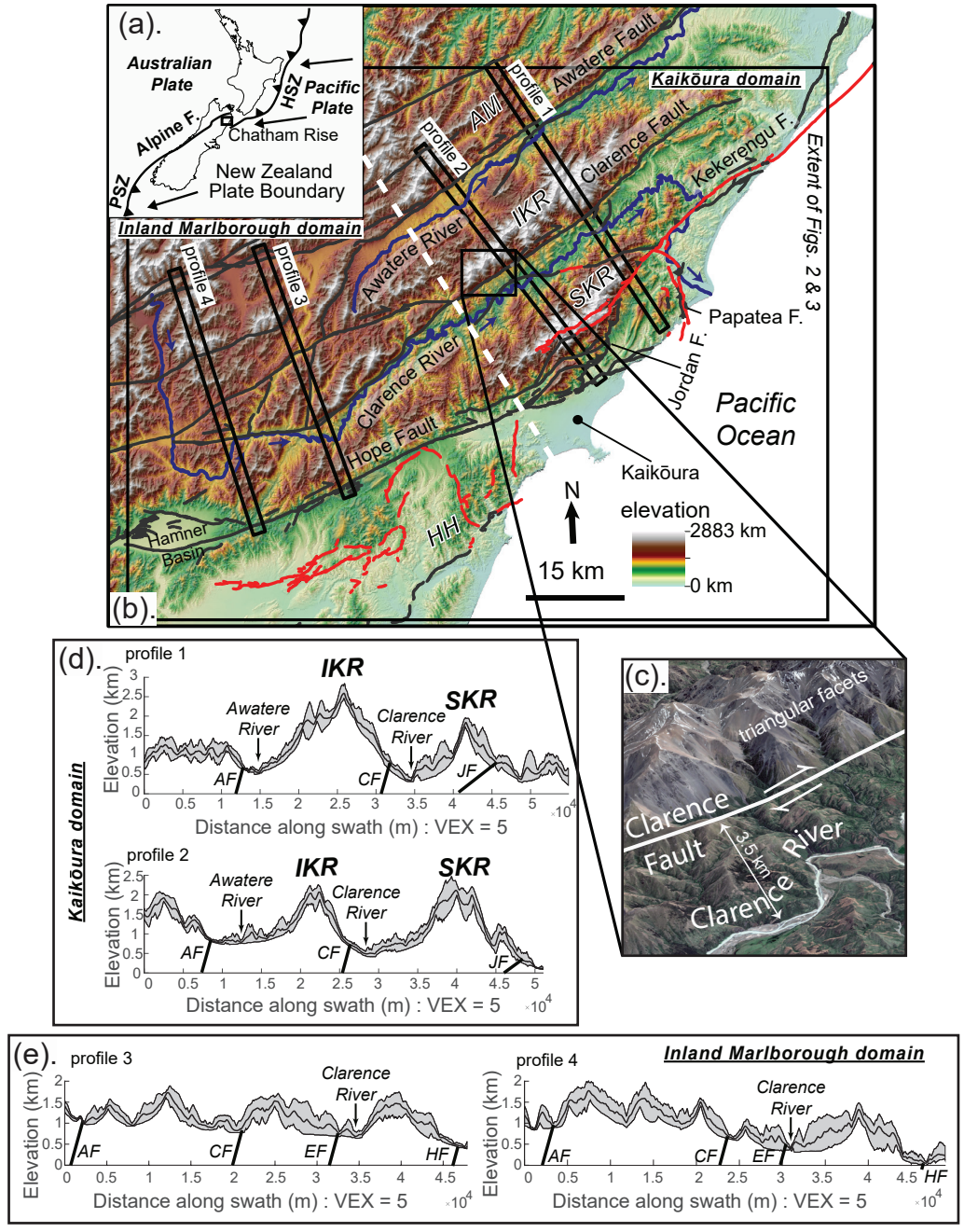

Figure 1: Field Site Location Map: Marlborough Fault System, New Zealand. (a) Inset shows New Zealand plate boundary. HSZ – Hikurangi Subduction Zone, PSZ – Puysegur Subduction Zone. Arrows show plate boundary convergence vectors (De Mets et al., 2010). (b) Shaded relief map created from 8 m resolution digital elevation map from Land Information New Zealand. Main stem rivers shown in blue, with arrows indicating flow direction. Active Faults (black) and faults that ruptured during the 2016 Kaikōura earthquake (red) from GNS Science fault database. White dashed line shows approximate boundary of the Inland Marlborough and Kaikōura domains. AW – Awatere Mountains, IKR – Inland Kaikōura Range, SKR – Seaward Kaikōura Range, HH – Hundalee

https://doi.org/10.5194/esurf-2019-41
Preprint. Discussion started: 7 August 2019

Earth Surface Dynamics Discussions
Open Access
EGU

Hills. (c) Blow up image of Clarence fault and Clarence river from Google Earth. Lower panels (d and e) show topographic swath profiles generated with the Topographic Analysis Kit (Forte and Whipple, 2019). Locations of profiles shown in main figure and labelled as profile 1, 2 (within Kaikōura domain) and 3,4 (within Inland Marlborough domain).

765

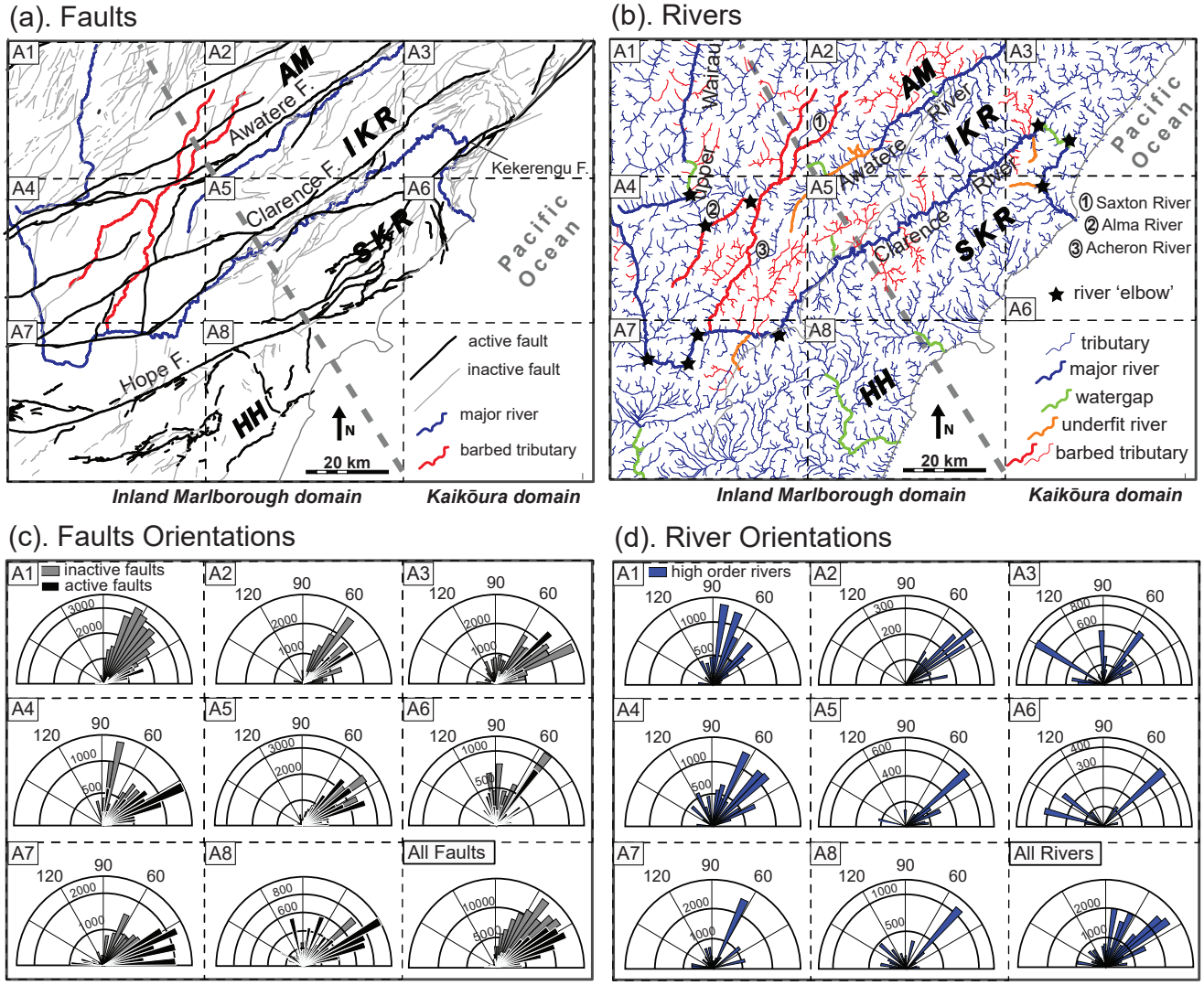

Figure 2: Marlborough Fault System planform fault and river patterns. (a) Map of field site faults (map extent shown in Fig. 1). Thicker line weight faults (black) are active faults in GNS database. Thinner line weight faults (gray) are inactive in GNS database. 770 **Main stem rivers shown in red/blue, same as in (b). (b) Map of field site showing rivers and drainage anomalies, same extent as (a). Main stem rivers shown in thicker line weight. Black stars are locations of river 'elbows' – places where the river bends ~ 90° degrees. AM – Awatere Mountains, IKR - Inland Kaikōura Range, SKR - Seaward Kaikōura Range, HH = Hundalee Hills. Half dial plots created using Topotoolbox2 (Schwanghart and Scherler, 2014) show 0 – 180° orientations of inactive (gray) and active (black) faults (c) and higher-order river segments (blue, d). Numbers within dials show the number of segments analyzed. Map area divided into** 775 **a grid of 8 boxes for spatial analysis of orientations. Locations of box A1 – A8 shown in (a) and (b).**

https://doi.org/10.5194/esurf-2019-41
Preprint. Discussion started: 7 August 2019

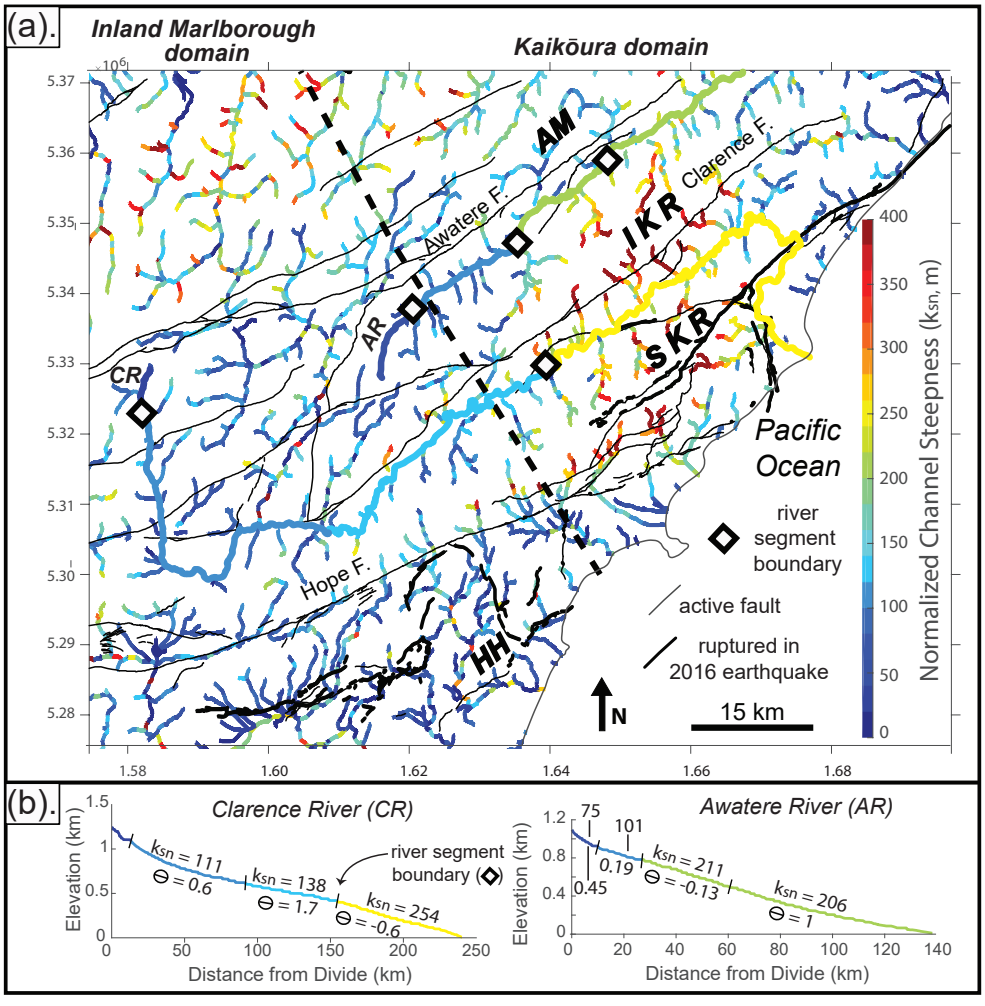

780

Figure 3: (a) Map of normalized channel steepness for study site channels. Map generated using the k_{sn} batch function in the Topographic Analysis Kit (Forte and Whipple, 2019). K_{sn} of main Awatere (AR) and Clarence (CR) river segments (heavier line weight) estimated from manual designation of segments on longitudinal channel profiles using the k_{sn} profiler function. Black dashed line divides the Inland Marlborough domain and the Kaikōura domain (b). Longitudinal river profiles of the Clarence and Awatere 785 **main stem rivers. Colors in b reflect the scale in a. k_{sn} - normalized channel steepness, θ - concavity, AM – Awatere Mountains, IKR - Inland Kaikōura Range, SKR - Seaward Kaikōura Range, HH = Hundalee Hills.**

https://doi.org/10.5194/esurf-2019-41
Preprint. Discussion started: 7 August 2019

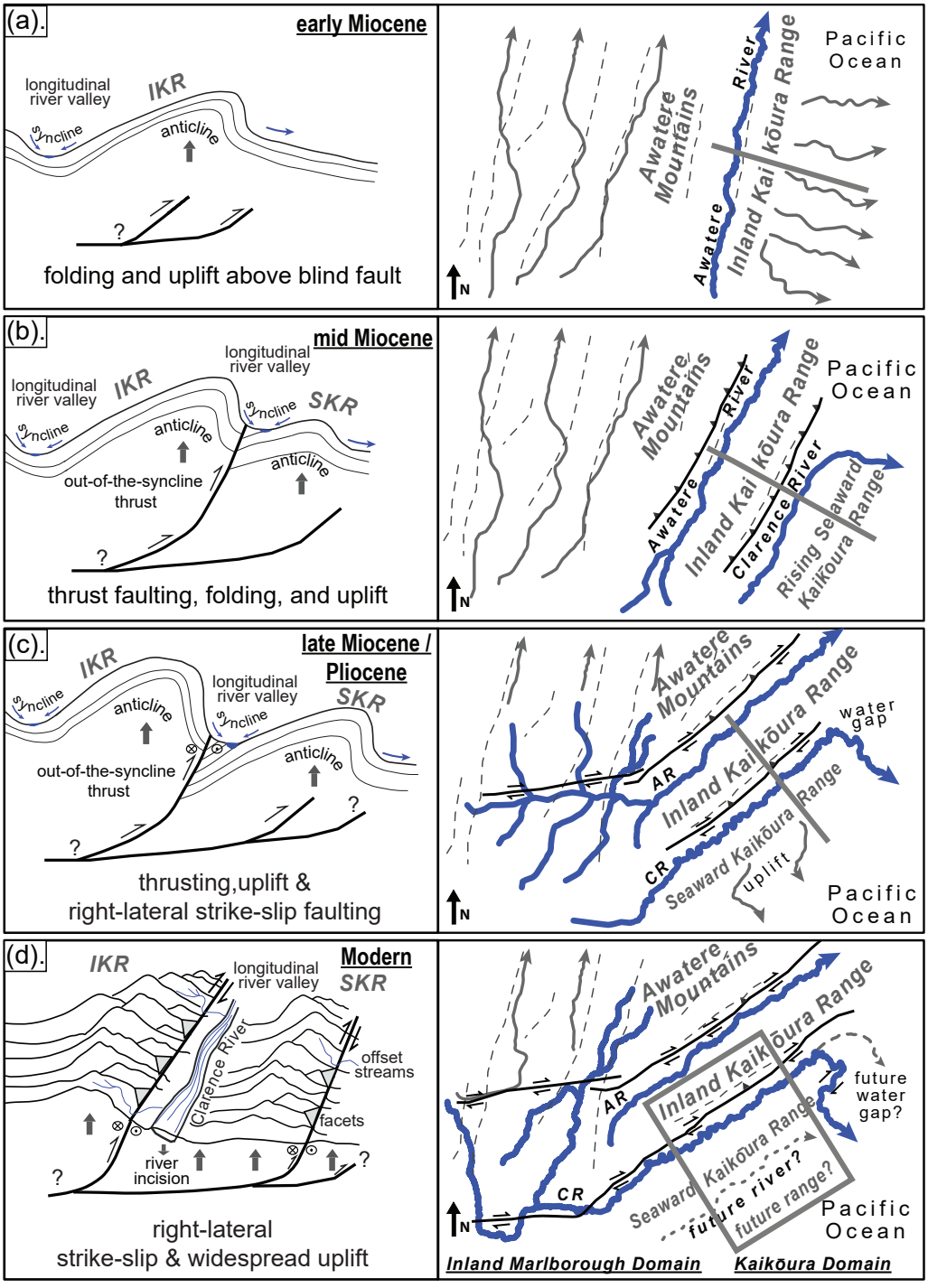

Figure 4: Schematic cartoon of Marlborough Fault System landscape evolution through time. Left panel shows cross-section view of the Kaikōura domain and right panel shows map view of landscape, expanded to include both the Kaikōura and Inland

https://doi.org/10.5194/esurf-2019-41
Preprint. Discussion started: 7 August 2019

Earth Surface Dynamics Discussions
Open Access
EGU

Marlborough domains. Approximate location of left-panel cross section shown with gray line (a,b,c) or box (d) in right panel. Right panel depicts active faults in black and inactive faults in gray and the approximate rotation of the faults and landscape from Randall et al. (2011). See section 5 of text for a description of our conceptual model.

795